Low Cloud Type over the Ocean from Surface Observations. Part I: Relationship to Surface Meteorology and the Vertical Distribution of Temperature and Moisture

JOEL R. NORRIS*

Department of Atmospheric Sciences, University of Washington, Seattle, Washington

(Manuscript received 10 October 1996, in final form 4 June 1997)

ABSTRACT

Surface cloud observations and coincident surface meteorological observations and soundings from five ocean weather stations are used to establish representative relationships between low cloud type and marine boundary layer (MBL) properties for the subtropics and midlatitudes by compositing soundings and meteorological observations for which the same low cloud type was observed. Physically consistent relationships are found to exist between low cloud type, MBL structure, and surface meteorology at substantially different geographical locations and seasons. Relative MBL height and inferred decoupling between subcloud and cloud layers are increasingly greater for stratocumulus, cumulus-under-stratocumulus, and cumulus, respectively, at midlatitude locations as well as the eastern subtropical location during both summer and winter. At the midlatitude locations examined, cloudiness identified as fair-weather stratus often occurs in a deep, stratified cloud layer with little or no capping inversion. This strongly contrasts with cloudiness identified as stratocumulus, which typically occurs in a relatively well-mixed MBL under a strong capping inversion at both midlatitude and eastern subtropical locations. At the transition between subtropics and midlatitudes in the western North Pacific, cloudiness identified as fair-weather stratus occurs in a very shallow layer near the surface. Above this layer the associated profile of temperature and moisture is similar to that for cumulus at the same location, and neither of these cloud types is associated with a discernible MBL. Sky-obscuring fog and observations of no low cloudiness typically occur with surface-based inversions. These observed relationships can be used in future studies of cloudiness and cloudiness variability to infer processes and MBL structure where above-surface observations are lacking.

1. Introduction

Low clouds over the ocean play a key role in the global climate system because they have a much higher albedo than the underlying surface and therefore can greatly influence the surface and top-of-atmosphere energy budgets. For this reason they have the potential to exert strong feedbacks on climate variability and climate change, but the magnitude and even the sign of these feedbacks are not well known. General circulation models (GCMs) show significantly different responses to a change in climate forcing depending largely on the strength of cloud feedbacks in the model (Cess et al. 1990; Cess et al. 1996), which in turn depend on the cloud parameterizations. Since marine boundary layer (MBL) clouds in particular are generally poorly simulated by GCMs (e.g., Soden 1992), much effort has gone into better understanding the factors controlling the amount and optical thickness of low cloudiness. Field experiments such as the First ISCCP (International Satellite Cloud Climatology Project) Regional Experiment (FIRE) (Albrecht et al. 1988) and the Atlantic Stratocumulus Transition Experiment (ASTEX) (Albrecht et al. 1995a) have been conducted to investigate how MBL processes and the large-scale environment influence cloud properties and the transition between stratocumulus and trade cumulus cloud regimes in the eastern subtropical ocean. Although these and similar projects have produced a wealth of detailed information on the radiative and microphysical properties of clouds and the dynamical and thermodynamical properties of the MBL, the data exist only for short periods of time at a few locations and focus on the subtropical ocean. Thus, it is desirable to sample over longer time periods and in a greater variety of climate regimes, especially the midlatitude ocean.

Recent studies have examined relationships between seasonal, interannual, synoptic, and El Niño–Southern Oscillation variability in cloudiness and other climate parameters over the ocean (e.g., Deser and Wallace 1990; Hanson 1991; Tselioudis et al. 1992; Deser et al. 1993; Klein and Hartmann 1993; Oreopoulos and Davies 1993; Norris and Leovy 1994; Weare 1994; Klein et al. 1995; Weaver and Ramanathan 1996; Klein 1997). Although these investigations have obtained basic information about processes influencing cloudiness, their

*Current affiliation: National Center for Atmospheric Research, Boulder, Colorado.

Corresponding author address: Joel R. Norris, NCAR/ASP, P.O. Box 3000, Boulder, CO 80307-3000.
E-mail: jnorris@ucar.edu

FIG. 1. Locations of OWS B (56.5°N, 51°W), C (52.75°N, 35.5°W), N (30°N, 140°W), P (50°N, 145°W), and V (34°N, 164°E), which contributed soundings and surface observations for this investigation.

use of broad categories of cloud type, typically total cloud amount, limits their explanatory capability. For example, because an observed change in total cloudiness does not distinguish a change in cumulus cloudiness from a change in stratus cloudiness, it is difficult to specifically identify the factors responsible for the observed change in total cloudiness since cumulus and stratus form under very different conditions. Satellite-based cloud datasets such as ISCCP (Rossow and Schiffer 1991) are similarly limited in their ability to examine processes affecting low cloudiness since they cannot easily distinguish between low cloud types. For example, thin overcast stratus and thick patchy cumulus occur in MBLs with significantly different properties, but the ISCCP algorithm may encounter difficulty distinguishing between them if the cloud elements are smaller than the pixel size. This paper proposes that many of the previously described handicaps may be overcome by using a global dataset based on synoptic surface observations organized by individual cloud type. Although synoptic surface observations lack quantitative radiative measurements, they cover a much longer time period than do satellite observations, and the observers' identification of clouds by morphological type contains qualitative information about MBL structure.

Since synoptic surface observations of cloud type have not seen much previous use in climate research, the present pair of papers is intended to lay a general foundation for future specific investigations by demonstrating the general usefulness of synoptic surface observations of cloud type in providing information on the local MBL structure and meteorological conditions in several different climate regimes and seasons and by documenting climatological distributions of individual low cloud types as a baseline for future interannual studies. Part I presents the average vertical distributions of temperature and moisture associated with commonly occurring cloud types using ocean weather station (OWS) data (locations shown in Fig. 1). This is complementary to the work of Betts et al. (1995), Albrecht et al. (1995b), and Klein (1997), who focused on cloud fraction rather than cloud type. Composite soundings are constructed for stratocumulus, cumulus-under-stratocumulus, moderate and large cumulus, fair-weather stratus, bad-weather stratus, sky-obscuring fog, and no-low-cloud for several midlatitude and subtropical locations during summer and winter seasons. Mean surface meteorological parameters associated with the cloud types are also calculated to show how the local environment influences low cloud type. These observed relationships will be useful for interpreting the results of Part II, which presents the global distributions of the frequency of occurrence of all low cloud types for summer and winter seasons with additional illustrations of certain transitions in cloud type (Norris 1998).

2. Data

a. Cloud type

Synoptic surface cloud type observations are particularly useful for studying low cloudiness because human observers identify clouds by morphological type, which is qualitatively related to the dynamical and thermodynamical environment in which the clouds occur. Table 1 gives nontechnical descriptions of each low cloud type (including no-low-cloud) classified according to the synoptic code (WMO 1975) and the abbreviations that will be used in this paper. If more than one cloud type is present, certain cloud types have priority over others in designating the low type code (C_L) even if they cover only a small fraction of the sky (Table 1). Thus, if any cumulonimbus with anvil is present then $C_L = 9$, otherwise if any cumulonimbus without anvil is present then $C_L = 3$, etc. If only $C_L = 1$, 5, 6, or 7 are present, then the low type code is designated by whatever type has the greatest sky cover. If no low cloud is present, then $C_L = 0$. Occasionally it is not possible to observe low cloudiness due to sky-obscuring fog or sky-obscuring precipitation (diagnosed by the present-weather code), which are identified as two additional ''low cloud types'' for the purposes of this paper. These 12 types include every possible sky condition for low cloud identification.

Figure 2 shows the climatological frequency of occurrence of each low cloud type during June–August (JJA) and December–February (DJF) at 0000 UTC for OWS B and C and at 1200 UTC for OWS N, P, and V. These hours are the times of the nighttime sounding and correspond to 2036, 2138, 0240, 0220, and 2256 local time at OWS B, C, N, P, and V, respectively. Daytime observations are not used due to biases in sounding

TABLE 1. WMO low cloud classification.

C_L Code	Priority[a]	Nontechnical cloud type description
0	7	No stratocumulus, stratus, cumulus, or cumulonimbus
1 (small Cu)	6[b]	Cumulus with little vertical extent and seemingly flattened, or ragged cumulus other than of bad weather,[c] or both
2 (Cu)	5	Cumulus of moderate or strong vertical extent, generally with protuberances in the form of domes or towers, either accompanied or not by other cumulus or by stratocumulus, all having their bases at the same level
3	2	Cumulonimbus the summits of which, at least partially, lack sharp outlines, but are neither clearly fibrous (cirriform) nor in the form of an anvil; cumulus, stratocumulus, or stratus may also be present
4	3	Stratocumulus from the spreading out of cumulus; cumulus may also be present
5 (Sc)	6[b]	Stratocumulus not resulting from the spreading out of cumulus
6 (St)	6[b]	Stratus in a more or less continuous sheet or layer, or in ragged shreds, or both, but no stratus fractus of bad weather[c]
7 (Fs)	6[b]	Stratus fractus of bad weather[c] or cumulus fractus of bad weather, or both (pannus), usually below altostratus or nimbostratus
8 (Cu-under-Sc)	4	Cumulus and stratocumulus other than that formed from the spreading out of cumulus; the base of the cumulus is at a different level than that of the stratocumulus
9	1	Cumulonimbus, the upper part of which is clearly fibrous (cirriform), often in the form of an anvil, either accompanied or not by cumulonimbus without anvil or fibrous upper part, by cumulus, stratocumulus, stratus, or pannus

[a] 1 is highest priority and 7 is lowest priority in designating C_L if more than one type is present.
[b] If no C_L 2, 3, 4, 8, or 9 is present, priority is determined by whatever type has the greatest sky cover.
[c] ''Bad weather'' denotes the conditions that generally exist during precipitation and a short time before and after.

relative humidity. Table 2 shows the time periods for which good surface observations of clouds are available (with occasional missing data). Surface observers sometimes have difficulty identifying clouds on dark nights (Hahn et al. 1995). This is mainly a problem for the detection of middle and high clouds but also affects the identification of low cloud type (Rozendaal et al. 1995). Frequencies are therefore calculated separately for nights with and without sufficient moonlight or twilight (using the criterion of Hahn et al. 1995). All significant cloud types except cumulonimbus are well-sampled by these locations.

The cloud-type frequencies displayed in Fig. 2 are consistent with the season and climate regime at each OWS location. The midlatitude OWS (B, C, and P) experience significant synoptic activity with the corresponding occurrence of bad-weather stratus. Warm advection is more prevalent during summer and cold advection is more prevalent during winter. Correspondingly, stratiform cloudiness and fog are most common during summer, consistent with Klein and Hartmann (1993), but cumulus often occurs during winter, particularly at those locations closer to land where strong cold-air outbreaks are more common. OWS V is located at the transition between subtropics and midlatitudes in the western Pacific and experiences some synoptic activity, especially during winter, but subtropical cumulus is otherwise most common. Warm advection predominates during summer and cold advection during winter. OWS N is located in the eastern subtropical ocean where subsidence and trade winds dominate during summer and winter and is in the transition region between subtropical stratocumulus and trade wind cumulus (Klein et al. 1995). Because synoptic activity is minimal, cloud types other than stratocumulus and cumulus rarely occur. The geographical and seasonal variations of cloud types will be discussed in greater detail in Part II (Norris 1998).

b. Synoptic surface observations

The OWS datasets used in this investigation were obtained from the National Climatic Data Center in Asheville, North Carolina, and provide synoptic observations of cloudiness and surface meteorology every 3 h during the time periods recorded in Table 2. In addition to low cloud type, cloud information includes the fractional coverage of the low cloud layer. Coincident surface meteorological information includes sea surface temperature (SST), surface air temperature, wind direction, wind speed, and present weather. Goerss and Duchon (1980) indicate that daytime deck heating can introduce substantial biases into measurements of surface air temperature and the subsequent calculation of air–sea temperature difference ($\Delta T \equiv T_{\text{air}} - \text{SST}$), but this should not be a problem in the present study since only observations at the time of the nighttime sounding are used. The frequencies of drizzle, rain, snow, showers, and fog were obtained using present-weather codes identifying precipitation or fog at the time and location of the observation, and the categories were defined following Hahn et al. (1996).

c. Soundings

While surface observations of cloudiness and other meteorological parameters have been routinely taken

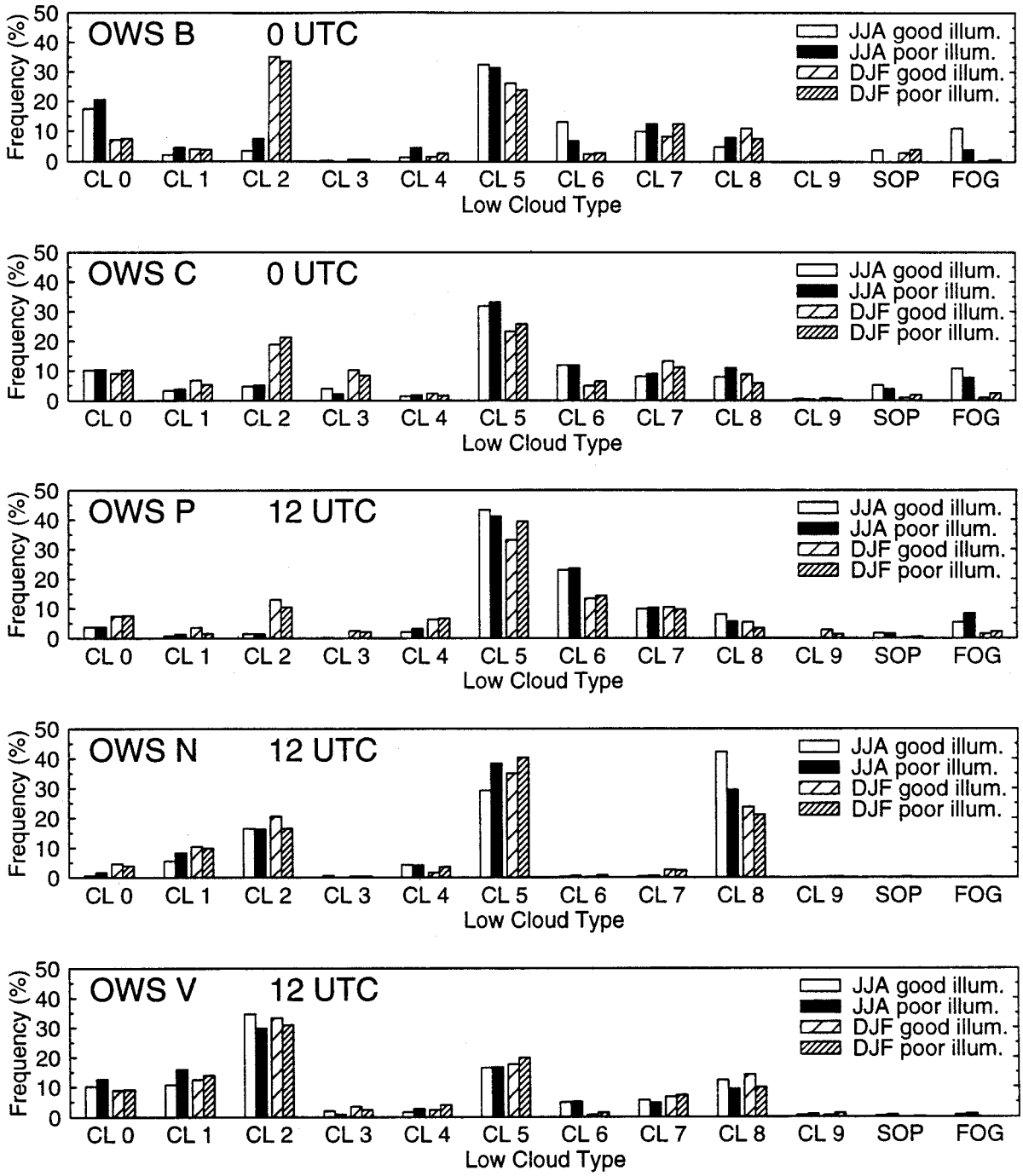

FIG. 2. Frequency of occurrence of the low cloud types described in Table 1 along with sky-obscuring precipitation (SOP) and sky-obscuring fog (FOG) at OWS B, C, N, P, and V during JJA and DJF. Observations are from 0000 UTC or 1200 UTC under conditions of good illumination and poor illumination according to the criterion of Hahn et al. (1995). Color coding of bar: white—JJA, good illumination; black—JJA, poor illumination; light hatching—DJF, good illumination; dense hatching—DJF, poor illumination.

over most of the global ocean for many decades, detailed information about the atmosphere above the surface is much more limited. The present investigation uses relatively high resolution soundings obtained from NCDC for OWS B, C, N, and V (OWS P has soundings only at 50-mb resolution). Most of the OWS operated for several decades until the early 1970s, and twice-daily soundings with coincident surface observations (described in the previous section) are available for most of that time period with occasional missing data. Un-

TABLE 2. Availability of good data.

	OWS B	OWS C	OWS N	OWS P	OWS V
Surface observations	Jan 54–Apr 74	Jan 54–Dec 87	Jan 54–Apr 74	Jan 54–Jun 81	Jan 54–Jan 72
Significant-level soundings	Jul 70–Jun 74	Jul 70–Dec 73	Jul 70–Jun 74	Not available	Jul 70–Jan 72
Number of JJA soundings*	254 (226)	299 (141)	249 (69)	0	149 (37)
Number of DJF soundings*	197 (51)	239 (80)	230 (71)	0	107 (39)

* The parentheses indicate the number of soundings with conditions of good illumination.

fortunately, prior to July 1970 the soundings were archived at 50-mb resolution, which is insufficient to accurately specify the depth of the MBL or the strength of the capping inversion. For the few remaining years (see Table 2) soundings were archived at significant levels (described in WMO 1974) and include data measured at or interpolated to every 50 mb as well.

Solar heating of the radiosonde hygristor caused daytime relative humidity to be substantially underestimated in the OWS soundings (Teweles 1970; Elliott and Gaffen 1991). The amount of underestimation varies with cloud cover and solar angle and consequently is impossible to correct in individual soundings. To avoid introducing an unknown humidity bias into the results, daytime OWS soundings were excluded from the analysis.[1] One drawback of this policy is that diurnal cycles in MBL decoupling (Betts 1990; Betts et al. 1995) that help drive diurnal cycles in cloud type (Klein et al. 1995; Rozendaal et al. 1995) will not be uniformly sampled. Furthermore, usually more than half of the nighttime cloud observations lack sufficient illumination.

Thin layers where potential temperature decreases substantially over a few meters are sometimes present in the OWS soundings. These almost always occur immediately above a nearly saturated layer at the base of the MBL inversion and are much more frequent in subtropical and summer soundings where cloud liquid water content is greater. Because the superadiabatic layers themselves are dry, the most likely explanation for this phenomenon is cooling of the thermistor due to the evaporation of droplets collected by the radiosonde while passing through a stratiform cloud at the top of the MBL. The sounding profiles were corrected by interpolating temperature between the base of the superadiabatic layer and the nearest level above the superadiabatic layer. No correction was applied to the lowest layer of the soundings because superadiabatic layers can sometimes occur at the surface if the SST is greater than the air temperature.

3. Compositing procedure

a. Selection of soundings

A composite sounding for a particular location and season was constructed by averaging the soundings for which the same low cloud type was reported at the time of the sounding. To increase the sample size, cloud observations made without sufficient illumination were included if the climatological frequency of occurrence of the reported cloud type under poor illumination did not exceed the frequency under good illumination at the 80% significance level for that location and season. For example, at OWS N during JJA it is likely that cumulus-under-stratocumulus (C_L 8)[2] is sometimes misidentified as ordinary stratocumulus (C_L 5) under conditions of poor illumination (Fig. 2). Therefore, all C_L 8 observations are accepted but poor-illumination C_L 5 observations are rejected. Table 2 shows the total number of soundings with coincident surface cloud observations at each location during JJA and DJF and also the number with good illumination. A few hundred soundings are available for each OWS but usually only a fraction have good illumination.

The fraction of soundings that can contribute to a composite depends on the frequency of occurrence of the cloud type. Since rare cloud types will have few soundings, only the more commonly occurring cloud types at each location and season are analyzed. Nonetheless, because the OWS occupy several different climate regimes nearly all cloud types except cumulonimbus are represented. Some cloud types have many soundings contributing; in these cases only the subset for which the cloud type had been persistent 3 h before and/or after the time of the sounding was used. This should improve the quality of the results by eliminating cases on the borderline between two cloud types. Additional improvement was obtained by removing a small fraction of soundings (typically 15%) that did not share the MBL structure commonly associated with the given cloud type. Although excluding such ambiguous soundings could be considered to bias the results, the practical result of including them is simply added noise, not change in the basic properties of the composite soundings. Nonetheless, it should be kept in mind that observers occasionally identify a particular cloud type under conditions not represented in the corresponding composite sounding. The number of soundings contributing to the composites at each OWS during each season

[1] June soundings at OWS B were still included in the analysis even though the sun is slightly above the horizon at 0000 UTC, but any solar heating should be negligible.

[2] The WMO description of C_L 8 merely states ''the base of the cumulus is at a different level than that of the stratocumulus'' (Table 1), but cumulus-under-stratocumulus is an appropriate paraphrase because stratocumulus-under-cumulus is unphysical.

TABLE 3. Number of significant-level soundings used in the composites, and means and standard deviations from Fig. 4.

	Number of soundings	MBL height (km)	$\delta q/q_s$(SST) ($\times$ 100)	ΔT (K)	S^* (K)
JJA OWS B C_L 5	33	0.67 ± 0.24	2.6 ± 12.2	−0.5 ± 1.0	19.0 ± 4.1
JJA OWS B C_L 8	7	0.92 ± 0.34	2.8 ± 10.8	−0.8 ± 0.8	14.8 ± 3.8
JJA OWS C C_L 5	46	0.86 ± 0.32	5.2 ± 8.5	−0.4 ± 1.2	18.7 ± 4.0
JJA OWS C C_L 8	12	1.13 ± 0.49	13.1 ± 11.1	−0.6 ± 0.9	15.6 ± 3.9
JJA OWS N C_L 5	7	1.26 ± 0.39	10.4 ± 5.9	−1.6 ± 0.8	18.3 ± 2.7
JJA OWS N C_L 8	68	1.67 ± 0.42	14.0 ± 6.5	−1.5 ± 0.8	17.3 ± 2.0
JJA OWS N C_L 2	15	1.88 ± 0.56	18.5 ± 7.6	−1.6 ± 0.9	16.6 ± 3.1
JJA OWS P C_L 5				−0.4 ± 0.8	17.3 ± 3.1
JJA OWS P C_L 8				−0.5 ± 0.7	15.5 ± 3.2
DJF OWS B C_L 5	11	1.14 ± 0.32	3.6 ± 7.0	−3.2 ± 2.3	11.0 ± 6.4
DJF OWS B C_L 8	18	1.67 ± 0.50	8.4 ± 11.2	−5.2 ± 3.7	4.5 ± 4.8
DJF OWS B C_L 2	20	2.07 ± 0.64	9.7 ± 6.7	−6.9 ± 3.4	0.3 ± 5.2
DJF OWS C C_L 5	12	1.26 ± 0.41	4.1 ± 7.0	−1.1 ± 2.0	14.5 ± 4.6
DJF OWS C C_L 8	17	1.66 ± 0.45	9.4 ± 9.2	−2.1 ± 1.8	9.5 ± 5.9
DJF OWS C C_L 2	13	2.61 ± 0.73	19.5 ± 10.6	−3.2 ± 2.1	3.9 ± 5.4
DJF OWS N C_L 5	17	1.37 ± 0.29	8.6 ± 7.1	−1.6 ± l.2	15.4 ± 2.5
DJF OWS N C_L 8	44	1.58 ± 0.34	11.9 ± 9.3	−1.7 ± 1.3	14.4 ± 2.4
DJF OWS N C_L 2	13	1.63 ± 0.54	17.0 ± 12.9	−1.6 ± 1.5	13.1 ± 3.5
DJF OWS P C_L 5				−0.6 ± 1.3	13.6 ± 7.1
DJF OWS P C_L 8				−1.9 ± 1.5	7.3 ± 6.0
DJF OWS P C_L 2				−2.3 ± 1.7	4.7 ± 5.2
DJF OWS V C_L 5				−1.5 ± 2.7	12.6 ± 3.8
DJF OWS V C_L 8	18	2.44 ± 0.79	15.3 ± 9.3	−2.8 ± 2.2	7.5 ± 4.4
DJF OWS V C_L 2	10	2.73 ± 1.16	18.9 ± 14.3	−3.5 ± 2.0	6.1 ± 4.8

* Stability.

are recorded in Tables 3 and 4. These numbers are not large enough for climatological significance, but the composites do show representative vertical distributions of temperature and moisture associated with particular cloud types. Moreover, the OWS soundings used in the composites are sampled from an entire season over a period of several years and thus have a much greater level of independence than those from short-term field projects (e.g., FIRE, ASTEX).

TABLE 4. Number of significant-level soundings used in the composites, and means and standard deviations from Fig. 6.

	Number of sound-ings	ΔT (K)	S^* (K)
JJA OWS B C_L 7	15	0.1 ± 1.0	18.3 ± 3.6
JJA OWS B C_L 0	12	0.7 ± 1.2	20.9 ± 3.7
JJA OWS B C_L 6	17	−0.1 ± 0.9	19.9 ± 3.9
JJA OWS B FOG	21	0.0 ± 1.2	23.6 ± 3.8
JJA OWS C C_L 7	29	0.2 ± 1.0	18.0 ± 4.1
JJA OWS C C_L 0	13	0.6 ± 1.0	19.9 ± 2.9
JJA OWS C C_L 6	28	0.2 ± 1.2	21.5 ± 3.5
JJA OWS C FOG	25	1.0 ± 1.0	23.7 ± 2.6
JJA OWS P C_L 7		0.0 ± 0.8	20.7 ± 3.5
JJA OWS P C_L 6		−0.1 ± 0.6	20.1 ± 3.4
JJA OWS P FOG		0.1 ± 0.9	21.3 ± 4.3
JJA OWS V C_L 2	22	−0.5 ± 1.0	14.2 ± 2.0
JJA OWS V C_L 0		0.3 ± 1.9	17.4 ± 2.6
JJA OWS V C_L 6	10	0.3 ± 1.1	18.6 ± 18

* Stability.

b. Scaling to MBL height

As noted by Albrecht et al. (1995b) and Klein et al. (1995), directly averaging temperature and moisture parameters on a pressure axis will smear out the sharpness of the capping inversion due to fluctuations in MBL height. To preserve the temperature and moisture structure at the top of the MBL all soundings were normalized by the height of the MBL prior to averaging. After averaging, the vertical axis of the composite sounding was rescaled to the mean MBL height. In all cases, MBL height was determined by visual inspection of the soundings.

For clouds occurring under capping inversions (stratocumulus and cumulus cloud types at OWS B, C, and N during summer and winter and OWS V during winter), MBL height was identified as the height of temperature minimum at the base of the inversion. This almost always corresponded closely to the base of the layer in which potential temperature began to increase substantially and both relative and specific humidity began to decrease substantially. In a few soundings the slope of potential temperature experienced a short decrease immediately above the apparent cloud top, suggesting spurious cooling due to the evaporation of cloud droplets off the radiosonde; in these cases MBL height was identified as the base of the layer where relative humidity began to decrease substantially. If there was no discernible temperature inversion (often the case for wintertime midlatitude cumulus), then the top of the

MBL was identified as the base of the layer where potential temperature began to increase substantially.

Sky-obscuring fog and no-low-cloud at OWS B and C occur with surface-based inversions; their soundings were normalized by the height of the temperature maximum at the top of this inversion. Fair-weather stratus at OWS B and C typically has a clearly defined cloud top but often occurs without a clearly defined capping inversion or stable layer. For this reason fair-weather stratus soundings were normalized by the height at which relative humidity began to significantly decrease with height. Bad-weather stratus at all locations and cumulus and stratus at OWS V during summer-typically did not have MBLs that could be clearly defined by either potential temperature or relative humidity; their soundings were not normalized.

c. Surface observations and 50-mb sounding data

Surface observations of low cloud fraction, SST, ΔT, wind speed, zonal and meridional wind components, and frequencies of fog and various precipitation types, were averaged for each cloud type over the entire multidecadal time period. The lower-tropospheric static stability, $S \equiv \theta(700\text{ mb}) - \theta(\text{SST, SLP})$, was averaged for each cloud type using the entire sounding data set. However, a slightly different definition of S from that of Klein and Hartmann 1993) was used where SST is substituted for surface air temperature. Only observations at the time of day of the nighttime sounding made under conditions of sufficient sky illumination were averaged. To obtain more distinctive results, observations were averaged only when the cloud type had been persistent 3h before and after the observation. When less than 40 observations were available, the persistence criterion was relaxed to allow more observations to contribute.

4. Results

a. Clouds under capping inversions

A temperature inversion almost always caps the MBL over eastern subtropical oceans and frequently caps the MBL over midlatitude oceans, particularly during summer (Klein and Hartmann 1993). Subsidence associated with the subtropical anticyclone promotes inversions over the eastern subtropical ocean and probably contributes to inversions over the midlatitude ocean during summer, and subsidence behind a cold front probably promotes inversions over the midlatitude ocean during winter and contributes to inversions during summer. Much recent research has been devoted to understanding physical processes controlling cloud amount in inversion-capped MBLs with a particular focus on the transition from stratocumulus to trade cumulus in the eastern subtropical ocean (e.g., ASTEX). The conceptual model of Bretherton (1992) and Wyant et al. (1997) proposes that a generally well-mixed MBL with stratocumulus becomes increasingly decoupled as it is advected by the trade winds over increasingly warm SST. In a decoupled MBL (described by Nicholls 1984) intermittent cumuli carry moisture from the subcloud layer to the cloud layer to maintain the stratocumulus deck. In a more strongly decoupled MBL, entrainment may evaporate the stratocumulus deck leaving only cumulus in the cloud layer. The present investigation indicates that the occurrence of cumulus-under-stratocumulus and cumulus with increased MBL height and inferred increased decoupling is true not only in the eastern subtropical ocean but also at midlatitudes during both summer and winter.

Figure 3 shows composite vertical distributions of water vapor mixing ratio (q), saturation water vapor mixing ratio (q_s), virtual potential temperature (θ_v), and equivalent potential temperature (θ_e) for stratocumulus (C_L 5), cumulus-under-stratocumulus (C_L 8), and moderate and large cumulus (C_L 2) at OWS N during JJA and OWS C during JJA and DJF (no composite is shown for cumulus at OWS C during JJA since it rarely occurs). Composite soundings for OWS N during DJF (not shown) are similar to those during JJA and composite soundings for OWS B (not shown) are similar to those for OWS C. Stratocumulus and cumulus cloud types at these locations almost never occur except under an inversion and vice versa. The capping inversion is strongest over the eastern subtropical ocean and weaker at midlatitudes, especially during winter when the top of the MBL is often defined by a substantial increase in θ_v with little increase in temperature. Although the large-scale environments at the locations and seasons displayed in Fig. 3 are different, each set of soundings shares common features. The depth of the MBL and the increase in θ_v and decrease in q within the MBL above the surface layer increases from stratocumulus to cumulus-under-stratocumulus to cumulus.

Inspection of soundings coincident with observations of cumulus-under-stratocumulus and cumulus cloudiness from the ASTEX R/V *Valdivia* (not shown) indicates most of the change in stratification and humidity within the MBL above the surface layer frequently occurs in a single jump near the middle of the MBL, similar to the case for the trade wind MBL reported by Augstein et al. (1974). Unfortunately, the OWS significant level soundings lack sufficient resolution to discern a jump in θ_v and q between a decoupled cloud layer and subcloud layer, but the ASTEX soundings suggest that the change in stratification and humidity within the MBL seen by the OWS may often result from decoupling. Since the best measure of decoupling is probably the decrease in q from subcloud layer to cloud layer (C. Bretherton 1997, personal communication), the parameter $\delta q \equiv q(z/z_i = 0.2) - q(z/z_i = 0.9)$, where z_i is the height of the MBL, is introduced. These are the same locations in the MBL that Albrecht et al. (1995b) chose to sample in the subcloud layer and near the top of the cloud layer. Because the present study focuses on the differences in δq between cloud types and not the ab-

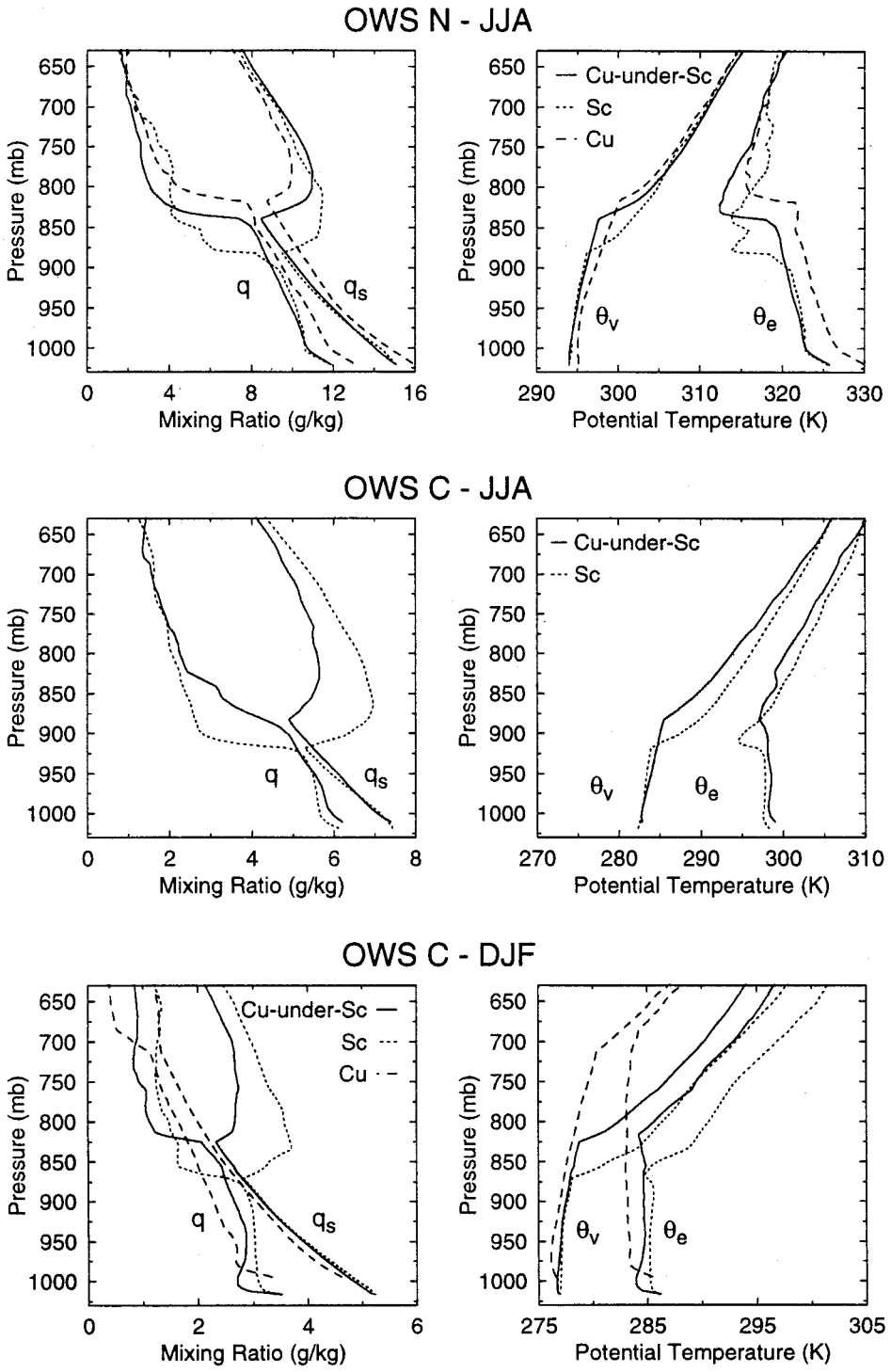

FIG. 3. Composite water vapor mixing ratio (q) and saturation water vapor mixing ratio (q_s) (left) and virtual potential temperature (θ_v) and equivalent potential temperature (θ_e) (right) for cumulus-under-stratocumulus (C_L 8) (solid), stratocumulus (C_L 5) (dotted), and moderate and large cumulus (C_L 2) (dashed) at OWS N during JJA (top), OWS C during JJA (middle), and OWS C during DJF (bottom).

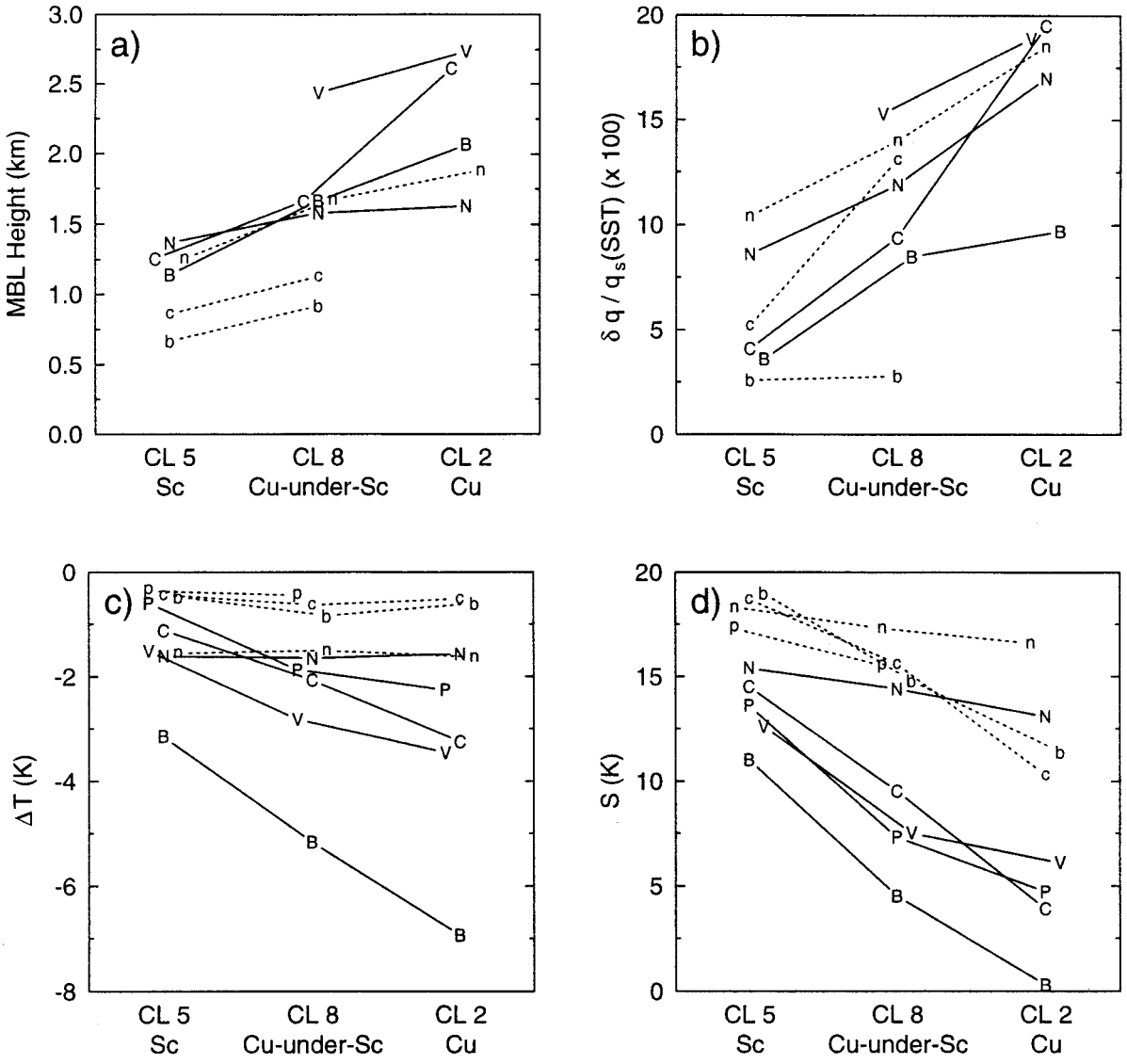

FIG. 4. (a) MBL height from significant-level sounding composites, (b) $\delta q/q_s$(SST) from significant-level sounding composites, (c) ΔT from surface observations, and (d) S from 50-mb resolution soundings for stratocumulus (C_L 5), cumulus-under-stratocumulus (C_L 8), and moderate and large cumulus (C_L 2). OWS locations are identified by letter for DJF (uppercase and solid lines) and JJA (lowercase and dotted lines). Some values have been slightly offset along the x axis to improve readability.

solute values of δq, the conversion of water vapor to liquid water will not bias the results unless cloud liquid water in the sounding profiles increases with decoupling. This is unlikely to be the case since the stratocumulus deck is expected to be thinner for cumulus-under-stratocumulus than for stratocumulus alone, and only a fraction of the soundings pass through cumulus clouds. Although not shown, similar results are obtained using parameters based on θ_v and θ_e.

Figure 4 shows average MBL height, $\delta q/q_s$(SST), ΔT, and S for stratocumulus, cumulus-under-stratocumulus, and moderate and large cumulus occurring under an inversion for various locations and seasons. The lines (solid for DJF and dotted for JJA) connect values for each cloud type at a single location and season. Because a smaller δq could occur in the colder midlatitude MBLs simply due to the nonlinear Clausius–Clapeyron relationship, δq is normalized by the SST saturation water vapor mixing ratio. Table 2 records the means and standard deviations of the data displayed in Fig. 4. Although not shown, the distributions of δq often exhibited considerable skewness, with the tail toward greater magnitude. Although the mean conditions at a given location and season are different for each cloud type, the large standard deviations indicate that the cloud types may not be well separated in parameter space.

At every location and during every season, MBL height and normalized δq are less than or the same for

stratocumulus than for cumulus-under-stratocumulus and less than or the same for cumulus-under-stratocumulus than for moderate and large cumulus (Figs. 4a and 4b). These results are consistent with those of Betts et al. (1995), who composited *Valdivia* soundings according to cloud fraction and found that the change in θ_e within the MBL was greater for 10% cloud cover (likely cumulus) than for 80% cloud cover (likely stratocumulus). Similarly, soundings composited by Albrecht et al. (1995b) for several locations in the subtropical and tropical ocean, including the *Valdivia,* show that locations with deeper MBLs are associated with increased decoupling, decreased cloud cover, and increased cumulus frequency. The fact that similar associations between cloud type, increased decoupling inferred from δq, and increased MBL height are observed at midlatitudes during summer and winter as well as in the subtropics suggests this general relationship tends to occur whenever the MBL is capped by an inversion.

Figure 4c shows that the average ΔT associated with stratocumulus and cumulus cloud types at these locations and seasons is always negative, suggesting the presence of cold advection. This is certainly the case for the trade wind regime at OWS N; examination of coincident surface winds at the other OWS (not shown) indicates a tendency for stratocumulus and cumulus cloud types to occur with flow from the direction of cooler SST or cold continents. The study of Lau and Crane (1995), who composited ISCCP cloud data with analyses from the European Centre for Medium-Range Weather Forecasts, found that clouds of varying optical thickness with low tops are associated with cold advection and subsidence. Assuming no overlying higher clouds, a satellite would identify stratocumulus, cumulus-under-stratocumulus, and cumulus as clouds of varying optical thickness with low tops. A subsequent study by Lau and Crane (1997) using surface cloud observations confirms that stratocumulus and cumulus are most common in the cold-advection region west of the low center.

Little variation occurs in ΔT between stratocumulus and cumulus cloud types during summer at midlatitudes and year-round in the subtropics, but ΔT is most negative for cumulus and least negative for stratocumulus during winter at midlatitudes. Figure 3 shows that above-inversion temperature at midlatitudes during winter is also coldest for cumulus and least cold for stratocumulus, suggesting that the strength of cold advection and atmosphere–ocean temperature difference during winter has a large influence on cloud type. Satellite photographs of cold-air outbreaks suggest a transition from stratocumulus to cumulus cloudiness following a trajectory from the coast (Houze 1993), implying more negative ΔT for stratocumulus than for cumulus. However, none of the OWS appear close enough to a coast to sample this initial stratocumulus of a strong cold-air outbreak.

Klein and Hartmann (1993) documented that increased cloud amount of combined stratus, stratocumulus, and fog is associated with a greater lower-tropospheric static stability for both the seasonal cycle and interannual anomalies. Figure 4d shows that S is greatest for stratocumulus and least for cumulus at every location and during every season, suggesting that a large part of the relationship documented by Klein and Hartmann is due to the fact that stratiform cloud types occur more frequently when S is greater. A further contribution results from the fact that stratocumulus typically has greater cloud amount than cumulus-under-stratocumulus, which typically has greater cloud amount than cumulus (Table 2 of Part II). The observed relationship between low cloud type and S is consistent with increased subsidence promoting a shallower MBL (Schubert et al. 1979a) and warmer temperatures at 700 mb.

Although the relative order of MBL height and normalized δq with cloud type is similar at all OWS locations, significant variations occur geographically and seasonally that can be grouped into three regimes: trade wind (not near the coast), summer midlatitude, and winter midlatitude. The summer midlatitude MBL is much shallower than the trade wind MBL, suggesting greater subsidence, weaker entrainment-generating turbulence, or both. Based on $\delta q/q_s$(SST), the summer midlatitude stratocumulus MBL is more well mixed than the trade wind stratocumulus MBL, consistent with the shallower MBL depth at midlatitudes. The summer midlatitude ΔT is distinctly lower than the trade wind ΔT, which, along with the colder SST, contributes to a weaker latent heat flux. On the other hand, the large winter midlatitude ΔT contributes to a much stronger surface buoyancy flux, which contributes to the much deeper winter midlatitude MBL (Schubert et al. 1979b).

b. Clouds not under capping inversions

A variety of structures occur when the MBL is not capped by a temperature inversion, such as surface-based inversions, strongly stratified layers, or weakly stratified layers. These three situations are illustrated in Fig. 5, which shows composite vertical distributions of q, q_s, θ_v, and θ_e for no-low-cloud (C_L 0), sky-obscuring fog, bad-weather stratus (C_L7), and fair-weather stratus (C_L6) at OWS C during JJA and moderate and large cumulus (C_L2) and fair-weather stratus at OWS V during JJA. Composite soundings for OWS B (not shown) are similar to those for OWS C. Composites are not shown for OWS N since the MBL there is rarely without a capping inversion. Figure 6 shows average ΔT and S for bad-weather stratus, no-low-cloud, fair-weather stratus, and sky-obscuring fog at various locations during JJA. Cumulus at OWS V is also included because it does not occur under an inversion. Note that S for stratus and fog is greater than that for cumulus at all OWS locations. Table 4 records the means and standard deviations of the data displayed in Fig. 6.

The extremely strong surface stratification, positive

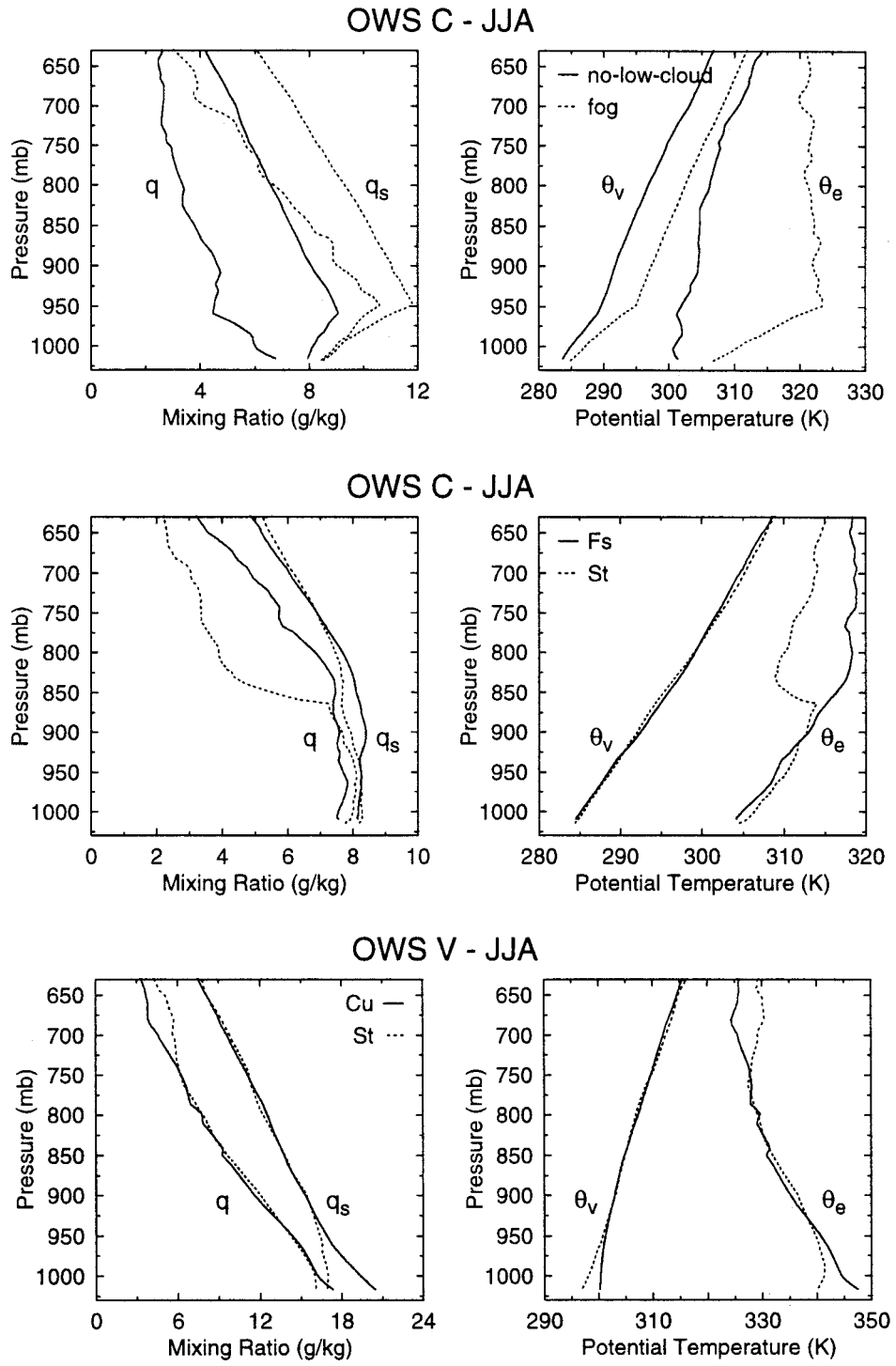

FIG. 5. As in Fig. 3 except for no-low-cloud (C_L 0) (solid) and sky-obscuring fog (dotted) OWS C during JJA (top), bad-weather stratus (C_L 7) (solid), and fair-weather stratus (C_L 6) (dotted) at OWS C during JJA (middle), and moderate and large cumulus (C_L 2) (solid) and fair-weather stratus (dotted) at OWS V during JJA (bottom).

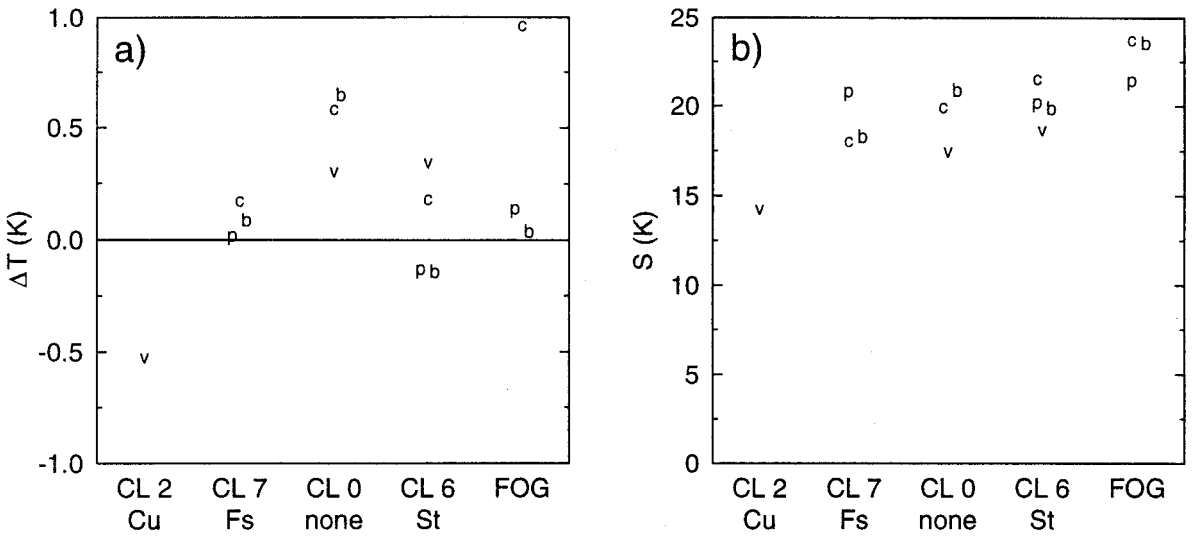

FIG. 6. (a) The ΔT from surface observations and (b) S from 50-mb resolution soundings for moderate and large cumulus (C_L 2), bad-weather stratus (C_L 7), no-low-cloud (C_L 0) fair-weather stratus (C_L 6), and sky-obscuring fog. OWS locations are identified by letter (JJA only). Some values have been slightly offset along the x axis to improve readability.

ΔT, large S, and strong southerly wind component (not shown) associated with observations of no-low-cloud and sky-obscuring fog at midlatitudes are consistent with strong advection of warmer air over colder water, as has been documented by previous studies of fog over the ocean (Taylor 1917; Tsukuda 1932). The no-low-cloud composite has much less low-level moisture than the sky-obscuring fog composite. Figure 14 of Part II (Norris 1998) shows that no-low-cloud generally occurs only very close to the coast, or sometimes poleward and eastward of continents at midlatitudes during summer. This suggests the occurrence of no-low-cloud at OWS B and C during summer corresponds to air masses of recent continental origin.

Fair-weather stratus at midlatitudes occurs in a saturated layer that is often shallow but sometimes quite deep, but bad-weather stratus usually has no clear MBL or cloud top and is nearly saturated through much of the troposphere. Fair-weather stratus frequently co-occurs with fog and drizzle, and bad-weather stratus is associated with particularly strong winds and substantial precipitation (not shown). The relatively large values of S, positive or slightly negative values of ΔT, and deep cloud layers suggest that fair-weather stratus as well as bad-weather stratus tends to be associated with warm advection and synoptic ascent. The fact that fair-weather stratus typically has a well-defined cloud top and largely occurs with drizzle whereas bad-weather stratus generally has no well-defined cloud top and largely occurs with rain suggests these two types differ by the degree of synoptic ascent. Although not shown, bad-weather stratus at midlatitudes during winter occurs with substantially warmer surface air temperatures than do the stratocumulus and cumulus types previously examined, and with precipitation that occurs predominantly as rain instead of snow. This suggests bad-weather stratus at midlatitudes during winter is also associated with warm advection. The study of Lau and Crane (1995) found that optically thick clouds with high tops, likely corresponding to nimbostratus, are associated with warm advection and ascent. Lau and Crane (1997) confirms that surface-observed nimbostratus is most frequent in the warm-advection region east of the low center.

The greatest difference between OWS V and the other OWS is the frequent lack of a discernible MBL or cloud top during the summer season, resulting from weaker or negligible subsidence at OWS V compared to the other locations. Furthermore, in contrast to the other locations, OWS V reported stratocumulus without a capping inversion a significant fraction of the time; for this reason stratocumulus soundings were not composited as was done at the other OWS. The synoptic context for stratocumulus at OWS V is not clear, but the associated soundings without an inversion bore some resemblance to those for stratus (not shown).

Both the moderate and large cumulus composite sounding and fair-weather stratus composite sounding at OWS V (bottom of Fig. 5) show a similar gradual decrease of temperature and humidity with height with the only difference being that the stratus composite is more saturated and stratified near the surface. This suggests that stratus at OWS V may often be associated with a very shallow, shear-driven stratus layer. The lack of an abrupt decrease in humidity in the cumulus composite suggests the cumuli have a broad distribution of cloud-top heights. In contrast to the other OWS, cumulus at OWS V during summer is associated with warm advection, and the difference between cumulus and stratus largely seems to depend on the SST associated with each (25.6°C for cumulus and 20.8°C for

stratus). This substantial difference in SST between cloud types does not occur at the other OWS and largely stems from cumulus replacing stratus as the strong SST gradient between subtropics and midlatitudes moves northward during summer (stratus is observed during June and July and cumulus is observed during July and August). Hence, the cumulus composite at OWS V may be viewed as corresponding to a location south of OWS V during June, and the stratus composite at OWS V may be viewed as corresponding to a location north of OWS V during August. In this sense, the stratus composite shows how the lower part of the cumulus composite is modified as it is advected from south to north over increasingly cold SST, along with a corresponding increase in S and change from negative to positive ΔT. This is consistent with Fig. 18 of Part II (Norris 1998), and the results of Norris and Leovy (1994), who found a strong negative correlation between interannual anomalies in seasonal mean stratiform cloudiness and SST in this region during JJA and attributed it to latitudinal shifts in the strong stratiform cloud and SST gradients that usually exist slightly north of OWS V. An equatorward shift in the region of strong SST gradient could produce significantly stronger warm advection at OWS V and result in more stratus compared to cumulus.

5. Conclusions

The preceding composite soundings and surface observations demonstrate the general consistency of synoptic surface observations of cloud type with the local meteorological conditions. Although the OWS data used in the present study sample only a few regions of the global ocean and have restricted statistical significance due to the limited number of soundings available, they provide representative information about the geographical and seasonal variability in the MBL structure associated with low cloud types as identified by the synoptic code. The physical consistency of the results suggests that the relationships documented in the present study can be used in subsequent work to qualitatively infer MBL structure and the synoptic environment from observations of low cloud type. However, the large standard deviations associated with many MBL and surface meteorological values indicates that some low cloud types may not be well separated in parameter space. Part II of this paper (Norris 1998) will show the geographical and seasonal variations of low cloud type over the global ocean.

Although the stationary observations at the OWS cannot track the evolution of individual MBL parcels, the examination of clouds under capping inversions suggests that transitions in cloud type between stratocumulus, cumulus-under-stratocumulus, and moderate and large cumulus are associated with changes in the relative depth and decoupling of the MBL over the midlatitude ocean as well as the eastern subtropical ocean. Observations of cumulus with stratocumulus by Nicholls (1984) and Norris (1998) imply that the MBL over the midlatitude ocean is frequently decoupled, suggesting it may be necessary for GCMs to account for MBL decoupling at midlatitudes to correctly simulate MBL cloudiness. Although the difference in cloud cover between ordinary stratocumulus and cumulus-under-stratocumulus is small (Norris 1998), the difference in cloud radiative forcing may be significant if the greater horizontal inhomogeneity of cumulus-under-stratocumulus due to the thinner stratocumulus cloud deck and underlying cumulus clouds (e.g., Klein et al. 1995) changes the mean albedo.

The large variety of conditions under which low clouds form, particularly at midlatitudes, indicate that investigations using broad categories of cloud types will have limited success in identifying processes responsible for changes in cloud amount. For example, the Warren et al. (1988) cloud atlas groups fair-weather stratus, bad-weather stratus, stratocumulus, cumulus with stratocumulus, and sky-obscuring fog together in the ''stratus'' category, but the present study shows that even fair-weather stratus can be very different from stratocumulus. Klein and Hartmann (1993) found a strong relationship between ''stratus'' cloud amount and S, but the present study indicates that this result occurs through distinctly different processes for stratus, stratocumulus, and sky-obscuring fog. Thus, parameterizations for stratus cloud amount based on simple relationships with S (e.g., Philander et al. 1996) are questionable, especially in regions where the stratus category is not dominated by a single cloud type. Further investigations into the processes responsible for cloud variability should be undertaken using datasets based on specific cloud type to resolve these issues.

Acknowledgments. This work was supported by an Earth Observing System Grant, NASA Grant NAGW-2633. The author wishes to thank Conway Leovy for his encouragement and support for this project, Stephen Klein for providing the OWS and ASTEX soundings and surface observations, and Bart Brashers for providing useful programs employed in the analysis. The author also appreciates useful comments from Conway Leovy, Stephen Klein, Christopher Bretherton, Bart Brashers, Stephen Warren, and an anonymous reviewer.

REFERENCES

Albrecht, B. A., D. A. Randall, and S. Nicholls, 1988: Observations of marine stratocumulus clouds during FIRE. *Bull. Amer. Meteor. Soc.,* **69,** 618–626.

——, C. S. Bretherton, D. Johnson, W. H. Schubert, and A. S. Frisch, 1995a: The Atlantic Stratocumulus Transition Experiment—ASTEX. *Bull. Amer. Meteor. Soc.,* **76,** 889–904.

——, M. P. Jensen, and W. J. Syrett, 1995b: Marine boundary layer structure and fractional cloudiness. *J. Geophys. Res.,* **100,** 14 209–14 222.

Augstein, E., H. Schmidt, and F. Ostapoff, 1974: The vertical structure of the atmospheric planetary boundary layer in undisturbed trade

winds over the Atlantic Ocean. *Bound.-Layer Meteor.,* **6,** 129–150.

Betts, A. K., 1990: Diurnal variation of the California coastal stratocumulus from two days of boundary layer soundings. *Tellus,* **42A,** 302–304.

——, C. S. Bretherton, and E. Klinker, 1995: Relation between mean boundary-layer structure and cloudiness at the R/V *Valdivia* during ASTEX. *J. Atmos. Sci.,* **52,** 2752–2762.

Bretherton, C. S., 1992: A conceptual model of the stratocumulus-trade-cumulus transition in the subtropical oceans. Preprints, *Proc. 11th Int. Conf. on Clouds and Precipitation,* Vol. I, Montreal, PQ, Canada, Amer. Meteor. Soc., 374–377.

Cess, R. D., and Coauthors, 1990: Intercomparison and interpretation of climate feedback processes in 19 atmospheric general circulation models. *J. Geophys. Res.,* **95,** 16 601–16 615.

——, and Coauthors, 1996: Cloud feedback in atmospheric general circulation models: An update. *J. Geophys. Res.,* **101,** 12 791–12 794.

Deser, C., and J. M. Wallace, 1990: Large-scale atmospheric circulation features of warm and cold episodes in the tropical Pacific. *J. Climate,* **3,** 1254–1281.

——, J. J. Bates, and S. Wahl, 1993: The influence of sea surface temperature gradients on stratiform cloudiness along the equatorial front in the Pacific Ocean. *J. Climate,* **6,** 1172–1180.

Elliott, W. P., and D. J. Gaffen, 1991: On the utility of radiosonde humidity archives for climate studies. *Bull. Amer. Meteor. Soc.,* **72,** 1507–1520.

Goerss, J. S., and C. E. Duchon, 1980: Effect of ship heating on dry-bulb temperature measurements in GATE. *J. Phys. Oceanogr.,* **10,** 478–479.

Hahn, C. J., S. G. Warren, and J. London, 1995: The effect of moonlight on observation of cloud cover at night, and application to cloud climatology. *J. Climate,* **8,** 1429–1446.

——, ——, and ——, 1996: Edited synoptic cloud reports from ships and land stations over the globe, 1982–1991. Carbon Dioxide Information Analysis Center Rep. NDP026B, 45 pp. [Available from Carbon Dioxide Information Analysis Center, Oak Ridge National Laboratory, P.O. Box 2008, Oak Ridge, TN 37831-6335.]

Hanson, H. P., 1991: Marine stratocumulus climatologies. *Int. J. Climatol.,* **11,** 147–164.

Houze, R. A., 1993: *Cloud Dynamics.* Academic Press, 573 pp.

Klein, S. A., 1997: Synoptic variability of low cloud properties and meteorological parameters in the subtropical trade wind boundary layer. *J. Climate,* **10,** 2018–2039.

——, and D. L. Hartmann, 1993: The seasonal cycle of low stratiform clouds. *J. Climate,* **6,** 1587–1606.

——, ——, and J. R. Norris, 1995: On the relationships among low-cloud structure, sea surface temperature, and atmospheric circulation in the summertime northeast Pacific. *J. Climate,* **8,** 1140–1155.

Lau, N.-C., and M. W. Crane, 1995: A satellite view of the synoptic-scale organization of cloud cover in midlatitude and tropical circulation systems. *Mon. Wea. Rev.,* **123,** 1984–2006.

——, and ——, 1997: Comparing satellite and surface observations of cloud patterns in synoptic-scale circulation systems. *Mon. Wea. Rev.,* **125**, 3172–3189.

Nicholls, S., 1984: The dynamics of stratocumulus: Aircraft observations and comparisons with a mixed layer model. *Quart. J. Roy. Meteor. Soc.,* **110,** 783–820.

Norris, J. R., 1998: Low cloud type over the ocean from surface observations. Part II: Geographical and seasonal variations. *J. Climate,* **11,** 383–403.

——, and C. B. Leovy, 1994: Interannual variability in stratiform cloudiness and sea surface temperature. *J. Climate,* **7,** 1915–1925.

Oreopoulos, L., and R. Davies, 1993: Statistical dependence of albedo and cloud cover on sea surface temperature for two tropical marine stratocumulus regions. *J. Climate,* **6,** 2434–2447.

Philander, S. G. H., D. Gu, D. Halpern, G. Lambert, N.-C. Lau, T. Li, and R. C. Pacanowski, 1996: Why the ITCZ is mostly north of the equator. *J. Climate,* **9,** 2958–2972.

Rossow, W. B., and R. A. Schiffer, 1991: ISCCP cloud data products. *Bull. Amer. Meteor. Soc.,* **72,** 2–20.

Rozendaal, M. A., C. B. Leovy, and S. A. Klein, 1995: An observational study of diurnal variations of marine stratiform cloud. *J. Climate,* **8,** 1795–1809.

Schubert, W. H., J. S. Wakefield, E. J. Steiner, and S. K. Cox, 1979a: Marine stratocumulus convection. Part I: Governing equations and horizontally homogeneous solutions. *J. Atmos. Sci.,* **36,** 1286–1307.

——, ——, ——, and ——, 1979b: Marine stratocumulus convection. Part II: Horizontally inhomogeneous solutions. *J. Atmos. Sci.,* **36,** 1308–1324.

Soden, B. J., 1992: Validation of cloud forcing simulated by the National Center for Atmospheric Research Community Climate Model using observations from the Earth Radiation Budget Experiment. *J. Geophys. Res.,* **97,** 18 137–18 159.

Taylor, G. I., 1917: The formation of fog and mist. *Quart. J. Roy. Meteor. Soc.,* **43,** 250–257.

Teweles, S., 1970: A spurious diurnal variation in radiosonde humidity records. *Bull. Amer. Meteor. Soc.,* **51,** 836–840.

Tselioudis, G., W. B. Rossow, and D. Rind, 1992: Global patterns of cloud optical thickness variation with temperature. *J. Climate,* **5,** 1484–1495.

Tsukuda, K., 1932: On the sea fog in the North Pacific Ocean. *Geophys. Mag.,* **6,** 147–165.

Warren, S. G., C. J. Hahn, J. London, R. M. Chervin, and R. L. Jenne, 1988: Global distribution of total cloud cover and cloud type amounts over the ocean. NCAR Tech. Note NCAR/TN-317+STR, Boulder, CO, 42 pp. plus 170 maps. [Available from National Center for Atmospheric Research, Boulder, CO 80307.]

Weare, B. C., 1994: Interrelationships between cloud properties and sea surface temperatures on seasonal and interannual time scales. *J. Climate,* **7,** 248–260.

Weaver, C. P., and V. Ramanathan, 1996: The link between summertime cloud radiative forcing and extratropical cyclones in the North Pacific. *J. Climate,* **9,** 2093–2109.

World Meteorological Organization, 1974: Manual on codes. WMO Publ. 306, WMO.

——, 1975: *International Cloud Atlas.* Vol. I. WMO Publ. 407, WMO, 155 pp.

Wyant, M. C., C. S. Bretherton, H. A. Rand, and D. E. Stevens, 1997: Numerical simulations and a conceptual model of the stratocumulus to trade cumulus transition. *J. Atmos. Sci.,* **54,** 168–192.